Pharm Res (2011) 28:3128–3144
DOI 10.1007/s11095-011-0503-9

RESEARCH PAPER

Disulfide Scrambling in IgG2 Monoclonal Antibodies: Insights from Molecular Dynamics Simulations

Xiaoling Wang • Sandeep Kumar • Satish K. Singh

Received: 14 March 2011 / Accepted: 31 May 2011 / Published online: 14 June 2011

ABSTRACT

Purpose To explore potential non-canonical disulfide linkages feasible in human IgG2 mAbs via molecular dynamics simulations of a model system, Hinge^{++}.

Methods Hinge^{++} is derived from the crystal structure of a full-length murine IgG2a antibody by replacing its core hinge region with human IgG2 hinge. Fv and C_H3 domains were discarded to speed up calculations. Eight independent simulations, grouped in four sets, were performed. In the control set, disulfide bonding is identical to canonical human IgG2 mAb. Different numbers of disulfide bonds were broken in the remaining three sets.

Results Two Fabs move towards Fc asymmetrically repeatedly leading to spatial proximity of LC.Cys214 and HC.Cys128 residues in one Fab with Cys residues in the upper hinge region, which could initiate disulfide scrambling. Local dynamics place the eight hinge region Cys residues in a large number of proximal positions which could facilitate non-canonical inter- and intra- heavy chain disulfide linkages in the hinge region.

Conclusion Consistent with experimental studies, our simulations indicate inter-chain disulfide linkages in human IgG2 mAbs are degenerate. Potential rational design strategies to devise hinge stabilized human IgG2 mAbs are gleaned.

KEY WORDS biotherapeutics · hinge · immunoglobulin · molecular modeling · structure

ABBREVIATIONS

CDR	complementarity-determining region
Fab	fragment antigen binding
Fc	fragment crystallizable
HC	heavy chain
LC	light chain
mAb	monoclonal antibody
MD	molecular dynamics
PDB	protein data bank
RMSD	root mean squared deviation

INTRODUCTION

The choice of antibody format is an important consideration for determining *in vivo* biological activity of a mAb therapeutic candidate (1). Most of the commercial therapeutic mAbs have been developed in IgG1/κ format. This format has proved extremely useful in the development of anti-cancer biotherapeutics due to the associated cell killing activities *via* effector functions located in the Fc portions of these antibodies. In many applications, however, the receptor binding is sufficient to achieve the therapeutic

Electronic Supplementary Material The online version of this article (doi:10.1007/s11095-011-0503-9) contains supplementary material, which is available to authorized users.

X. Wang · S. Kumar · S. K. Singh
Pharmaceutical Research and Development
BioTherapeutics Pharmaceutical Sciences, Pfizer Inc.
700 Chesterfield Parkway West
Chesterfield, Missouri 63017, USA

S. Kumar (✉)
BioTherapeutics Pharmaceutical Sciences Pfizer Inc.
MC6S, 575 Maryville Centre Drive
St Louis, Missouri 63141, USA
e-mail: Sandeep.Kumar@Pfizer.com

effect. The cytotoxic effector functions may not be required or may even be undesirable (2). Although the effector functions of IgG1 mAbs can be altered by mutations in the constant regions (3), IgG2 and IgG4 isotypes with reduced or nearly absent effector functions may be the desirable formats for such applications (2, 4). An increasing number of therapeutic mAb candidates in these formats, especially IgG2, are currently in various stages of development. Several modified forms of these isotypes have also been developed (5).

Both IgG2 and IgG4 show dynamic structural re-arrangements involving the hinge region disulfide bonds (6–10). This post-translational modification, termed disulfide scrambling, leads to structural heterogeneity in therapeutic human IgG2 mAbs. Disulfide scrambling may complicate the pharmaceutical development process and also potentially impact *in vivo* Fc domain involving biological activities of the therapeutic candidates (8). For example, IgG4 antibodies were found to form half molecules and exchange their Fab arms with endogenous IgG4 antibodies *in vivo* due to the conformational instability of the amino acid sequence CPSC in the hinge region. This may complicate the pharmaco- kinetic / dynamic studies involving IgG4 mAbs (6). The hinge region of IgG4 molecules can be conformationally stabilized by a single amino acid substitution of Ser with Pro, like in IgG1 and IgG2 hinges (CPPC) (6). Several disulfide isoforms have been detected for the human IgG2 antibodies (8, 9, 11, 12). Human IgG2 antibodies can also form dimers involving hinge region Cys residues and show increased avidity (13).

The sequence, structure, and arrangement of the intra- and inter-chain disulfide bonds for all IgG isotypes were deduced several decades ago (14–17). There are important differences in regard to the hinge region sequence and inter-chain disulfide bonding patterns among different IgG isotypes. For disulfide bonding patterns, these differences lie in the pairing of the light chain (LC) C-terminal Cys residue with a Cys residue in the heavy chain (HC) and the number of disulfide bonds present in the hinge region (1). However, these canonical disulfide pairing schemes are being re-examined in view of accumulating experimental evidence for inter-chain disulfide bond scrambling in the human IgGs (8, 9). The initial experimentally reported different disulfide isomers of human IgG2 antibodies involved the following Cys residues: C-terminal Cys residue in LC and its partner Cys in C_H1 domain of HC, and the two Cys residues in HC that form disulfide bonds in the upper hinge region (8, 9). These disulfide isomers are referred to as IgG2-A, IgG2-B, and IgG2-A/B (9). Figure 1 shows schematic diagrams of disulfide bonding schemes in different human IgG2 isoforms. IgG2-A, shown in Fig. 1a, is the canonical disulfide bonding pattern for human IgG2 mAbs (16). In this form, the LC C-terminal Cys forms a disulfide bond with the first Cys residue in the HC C_H1 domain. The hinge region contains four inter-heavy chain disulfide bonds, formed in register. In IgG2-B isoform (Fig. 1b), the disulfide bonding re-arrangement is symmetrical with respect to both the LC: HC and Fab: hinge pairs (8). Figure 1c shows an example of IgG2-A/B isoform (9). This isoform is a hybrid between IgG2-A and IgG2-B, and the disulfide linkage is asymmetric between the two LC: HC and Fab: hinge pairs. Subsequent experimental studies on human IgG2 disulfide scrambling have indicated that several different disulfide pairing schemes may exist under the umbrella of IgG2-B and IgG2-A/B isoforms (11, 18), and the diagrams shown in Fig. 1b and c are only one of the examples for each isoform. Moreover, disulfide scrambling may not be limited to the inter-chain Cys residues in Fab and the upper hinge portion. Zhang *et al.* have characterized novel variants of IgG2 disulfide isoforms containing intra-HC disulfide bonds in the lower hinge portion (12). Liu *et al.* have shown that the *in vivo* distribution of disulfide isomers of human IgG2 antibody is dynamic, i.e., the disulfide isoforms are interconvertible (10). Light chain type may influence the inter-conversion among the disulfide isoforms of an IgG2 antibody. IgG2-A form dominates in the antibodies with λ LC, while IgG2-B is predominant when LC type is κ (8, 9). Consistently, LC type was λ in the early experiments by Milstein and Frangione (16). Furthermore, efforts have been made to understand the contribution of specific Cys residues to disulfide scrambling *via* site-directed mutagenesis (19).

In light of the above information, there is a clear need to gain fundamental understanding of the dynamical nature of the hinge region and adjoining domains in human IgG2 mAbs and pin-point the determinants of inter-chain disulfide scrambling. This understanding should eventually facilitate rational structure-based approaches to mitigate or eliminate disulfide scrambling in therapeutic human IgG2 mAbs. Here, we have studied the disulfide scrambling in a model system that mimics the middle portion of human IgG2 mAb *via* multiple all-atom molecular dynamics (MD) simulations with explicit water molecules. We have followed the approach taken by van Gunsteren and coworkers to study disulfide scrambling in bovine α-lactalbumin and lipid transfer proteins (20, 21).

There is no publicly available crystal structure for full human IgG2 antibody. Here, we have used the crystal structure of a full-length murine IgG2a antibody (Protein Data Bank, PDB ID: 1IGT) (22, 23) to devise a molecular system we call Hinge^{++}. The details for this system are described in the Materials and Methods section. Briefly, the

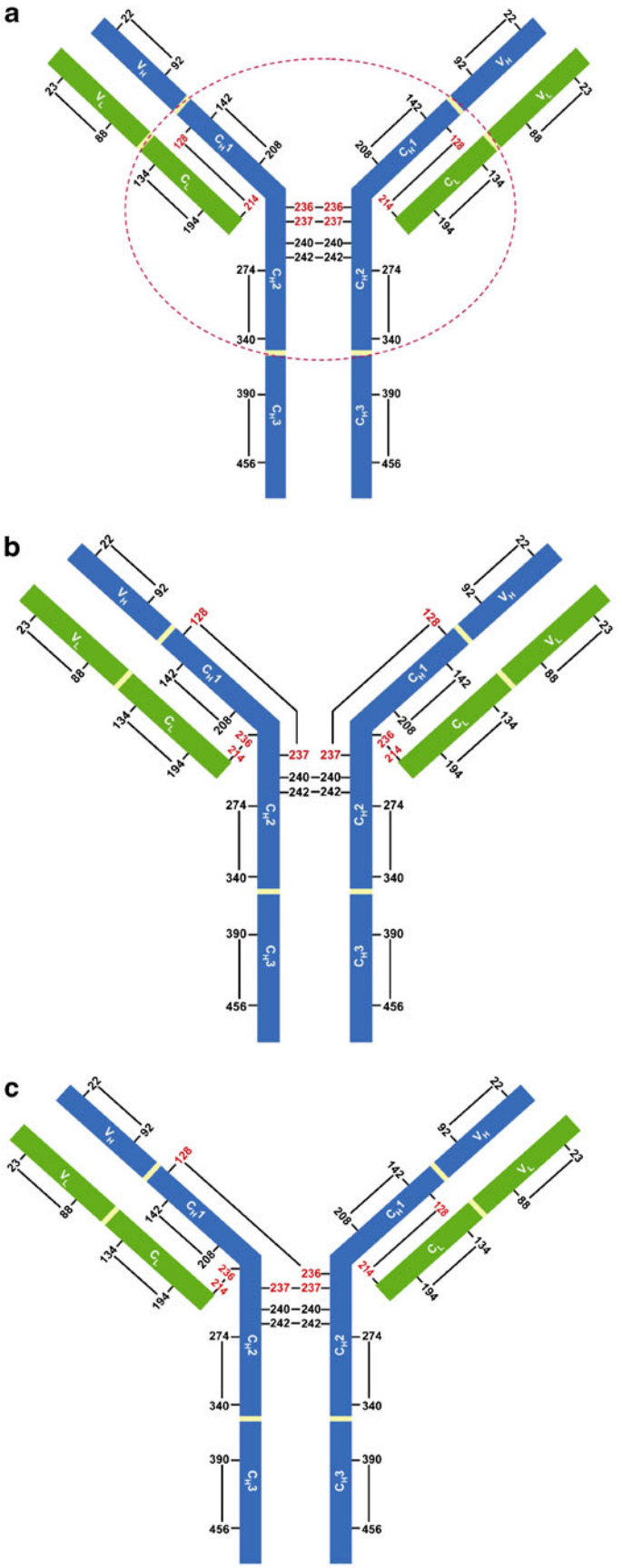

Fig. 1 Schematic representation of human IgG2 mAb. A human IgG2 mAb consists of two light chains (*green*) and two heavy chains (*blue*). The variable and constant domains of light chain are labeled as V_L and C_L, respectively. The four domains of heavy chain are labeled as V_H, C_H1, C_H2 and C_H3. The hinge which connects C_H1 and C_H2 is not explicitly labeled. All the disulfide bonds are explicitly shown together with the cysteine residue numbers. Numbering of cysteine residues follows the Kabat numbering used in 1IGT PDB structure. (**a**) IgG2-A disulfide isoform. This is the canonical IgG2 disulfide form established by Milstein *et al.* (16). The red dashed circle indicates the Hinge^{++} region that was subjected to dynamic simulations in this study. (**b**) A representative variant of IgG2-B disulfide isoform reported by Dillon *et al.* (Fig. 5 in Ref. 8) (8). Note cysteine residue numbering in our system is slightly different from that used by Dillon *et al.* (**c**) A variant showing IgG2-A/B isoform reported by Wypych *et al.* (Fig. 8 in Ref. 9) (9).

core hinge region of 1IGT was replaced with the one found in human IgG2 mAbs, and atomic coordinates of Fv and C_H3 domains were discarded. Using Hinge^{++}, we have performed four sets of all-atom explicit water molecular dynamics simulations. Each set contains two independent simulations. Each simulation is at least 20-nanosecond (ns) long. The first set consists of control simulations where all Cys residues are kept disulfide bonded as in the canonical IgG2-A form (Fig. 1a). The second set of simulations has all Cys residues reduced, that is, all the disulfide bonds are broken. The third one has all the six inter-chain disulfide bonds broken. Finally, the fourth set contains simulations with four inter-chain disulfide bonds broken. Two of these inter-chain disulfide bonds connect light and heavy chains. The remaining two disulfide bonds are in the upper hinge region. This set of simulations retains the two inter-chain disulfide bonds in the lower hinge region.

All simulations show that radius of gyration of Hinge^{++} decreases over simulation time, and closer inter-domain contacts are formed across the hinge region. High mobilities for the inter-chain disulfide bond-forming Cys residues are observed. The sulphur atom distances show large fluctuations for the Cys residue pairs originally involved in the canonical inter-chain disulfide bonds. In contrast, these distances are stable for intra-chain disulfide bond-forming Cys residue pairs. In particular, our simulations indicate that the light chain C-terminal Cys residue (Cys214) and the heavy chain Cys residue at the N-terminal of C_H1 domain (Cys128) could approach heavy chain Cys residues in the upper hinge region. These events could initiate disulfide scrambling in human IgG2 mAbs. Interestingly, contact map analyses indicate that Cys residues in the hinge region come frequently in contact with their non-canonical Cys residue partners. Overall, these atomistic simulations have provided several additional insights into the dynamics of hinge region and inter-chain disulfide pairing in human IgG2 mAbs which could not be gleaned from experiments alone. Rational strategies to design hinge-stabilized human IgG2 mAbs are formulated based on these simulations.

MATERIALS AND METHODS

Structural Model Building of Hinge^{++}

No crystal structure for full human IgG2 antibody is publically available so far. To overcome this limitation, we have replaced the core hinge region in the crystal structure of a full murine IgG2a antibody (PDB ID: 1IGT) (23, 24) with human IgG2 hinge *via in silico* modeling. This procedure was performed using the homology model module in MOE from the Chemical Computing Group (http://www.chemcomp.com/) and is described below.

We strived to minimize the potential errors due to homology modeling by making only minimal changes in the original crystal structure (1IGT). The following procedure was used. a) The changes in 1IGT were restricted to the core hinge region. The rest of the sequence and structure of 1IGT remained unchanged. b) 1IGT contains three inter-HC disulfide bonds in the hinge region, whereas the canonical human IgG2 antibody (A form) contains four inter-HC disulfide bonds. We preserved all three inter-HC disulfide bonds in 1IGT and created only one additional inter-HC disulfide bond. Figure 2a shows the sequence alignment of 1IGT hinge with human IgG2 core hinge used in this study. The sequence for the human IgG2 core hinge is ERKCCVECPPCP. A few murine antibody residues flanking the core hinge are also shown in the Fig. 2a. This alignment was performed manually. It differs significantly from the one obtained by the sequence alignment programs (Fig. 2b). Even though the automated alignment preserves and aligns the "CPPC" motif in the human and murine hinges, it would have required greater changes in the hinge of 1IGT. Therefore, the alignment in Fig. 2b was not adopted. By adapting the manual

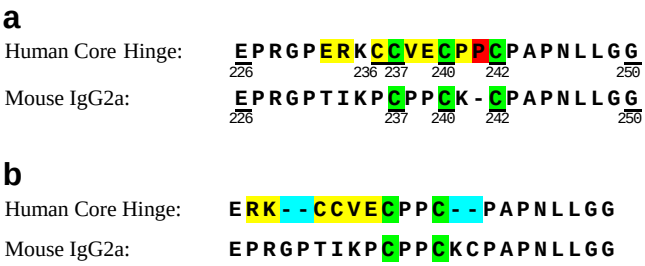

Fig. 2 Sequence alignment between the core hinge region of the murine IgG2a antibody 1IGT and the human core hinge region. Sequence shown includes the core hinge region as well as upper and lower hinge region. The core hinge sequence of human IgG2 is ERKCCVECPPCP. The residues flanking the human core hinge region are from 1IGT. (**a**) Sequence alignment used in the homology modeling. The replacement of murine core hinge region in 1IGT with human core hinge involves mutation of six residues and insertion of one residue. The mutated residues are highlighted in yellow. The inserted residue is highlighted in red. Green highlights the preserved Cys residue pairs whose inter-chain disulfide bonds in crystal structure are retained. Kabat numbering used in 1IGT PDB structure is followed. The residue numbers of the termini and cysteine residues are labeled. The two proline residues between C240 and C242 are numbered as 241 and 241a (not shown), respectively, in order to make the sequence numbering identical to the wild type murine sequence. (**b**) Sequence alignment generated by sequence alignment program. The sequence with human core hinge region is on the top. The motif "CPPC" is preserved in this alignment. However, the homology modeling using this alignment would have required greater changes including four residue deletions highlighted in blue. In the two alignments, the hinge sequences of 1IGT used are the same, but the number of residues flanking to human core hinge are different.

alignment shown in Fig. 2a, we were able to preserve all three inter-chain disulfide bonds in the hinge region of 1IGT. But this alignment also necessitated that we take CPPC motif out of register and mutate the Proline residues (Fig. 2a). Overall modification of 1IGT hinge region involved mutations at six residues positions, an insertion and creation of one inter-HC disulfide bond (Cys236-Cys236). The numbering of Cys residues is shown in Fig. 2a. Kabat numbering used in 1IGT PDB structure is followed throughout this study. Note that the hinge regions of antibodies are highly mobile and poorly defined in all the three publically available crystal structures for full length antibodies (PDB entries: 1IGT, 1IGY and 1HZH). The B-factors for hinge region residues in these crystal structures are substantially higher than the other regions.

The homology modeling process involved the following steps. 1) 1IGT crystal structure was used as the structural template. The target sequence is 1IGT sequence with its core hinge region replaced by human IgG2 core hinge (Fig. 2a). 2) One thousand intermediate homology models were generated and optimized by energy minimization. 3) The top ranked model was chosen. This model lacked the additional inter-HC disulfide bond (Cys236-Cys236) in the hinge region. The Cys236 side chain rotamer which yielded the smallest Cys236-Cys236 sulphur atom distance was chosen, and a Cys236-Cys236 disulfide bond was then created. 4) The hinge region was optimized via energy minimization while keeping the rest of molecule fixed. The whole molecule was then energy minimized without restraints.

Hydrogen atom positions were generated using MOE. All-atom AMBER99 forcefield was used in homology modeling and all energy minimization steps. A cut-off of 12 Å with switching started at 10 Å was applied to non-bonded interactions. Generalized Born implicit solvation was employed. Interior and exterior dielectric values were 4 and 80, respectively.

The above exercise yielded a structural model for a mouse antibody with human IgG2 core hinge. The conformations for greater than 99% of the residues in the crystal structure of 1IGT are retained in this model. The disulfide bonding scheme in this model is identical to the canonical human IgG2 structure (A form). For clarity, the two light chains named as chain A and chain C in 1IGT PDB are renamed as light chain 1 (LC1) and light chain 2 (LC2), respectively, throughout this study. Similarly, the two heavy chains, chain B and chain D, are renamed as heavy chain 1 (HC1) and heavy chain 2 (HC2), respectively. The Fab containing LC1, V_H and C_H1 domains of HC1 is named as Fab1, and the other Fab is named as Fab2.

The carbohydrate molecule attached to the C_H2 domain in 1IGT crystal structure was not included in the homology model and in the molecular dynamic simulations. We do not expect de-glycosylation would have a major impact on disulfide scrambling. The crystal structure of a monomeric un-glycosylated IgG1 C_H2 domain was reported by Prabakaran *et al.* (25). The authors found that C_H2 domain conformation remained very similar to the conformations of the corresponding glycosylated C_H2 domains from the crystal structures of Fc, full length IgG and Fc- receptor complexes. In a separate study, we have performed MD simulations on full length antibody in the PDB entry 1IGT in both glycosylated and un-glycosylated forms (data not shown). The hinge region dynamics are very similar in both forms. They are also very similar to the hinge region dynamics in the $Hinge^{++}$ system. Hence, absence of glycosylation in the $Hinge^{++}$ system is not anticipated to impact our results except for minor conformational differences in the C_H2 domains.

Experimental evidence indicates that disulfide scrambling is limited to inter-chain disulfide bonds which reside in the central region of antibody (8, 9, 11). In a separate study, we had created molecular models for a full human antibody in different disulfide isoforms (A, A/B and B) as described by Wypych *et al.* (9). The conformations of Fv and C_H3 domains, which do not contain inter-chain disulfide bonds, remained the same in all the three isoforms (C_α RMSD < 0.5Å). Another separate set of molecular dynamic simulations on full length antibody (1IGT) showed very similar overall dynamic profiles as in the $Hinge^{++}$ system. Hence, we have discarded the Fv and the C_H3 domains to reduce the computational cost for molecular simulations.

The 'truncated' molecular system was named $Hinge^{++}$. This molecular system consists of murine C_H1, C_H2 and C_L domains with the core hinge region being human. It contains four structural regions (Fig. 1a). These regions are 1) truncated Fab1 (tFab1) containing only the constant domain of Fab1; 2) truncated Fab2 (tFab2) containing only the constant domain of Fab2; 3) the hinge region (sequence region shown in Fig. 2a of both heavy chains); 4) the truncated Fc (tFc) containing the C_H2 domains of both heavy chains. $Hinge^{++}$ contains six intra-chain and six inter-chain disulfide bonds (Fig. 1a).

The $Hinge^{++}$ model should adequately represent the middle portion of a human IgG2 antibody, even though it is not a full model of a human IgG2 antibody. Sequence identities between a murine IgG2a mAb (1IGT) and fully human IgG2κ Panitumumab are 60% and 62% for the constant regions of light and heavy chains, respectively. The sequence identities for the corresponding C_H1 domains and C_H2 domains are 64% and 67%, respectively. The structural conservation is even stronger because the individual domains of IgG molecules share the ancient immunoglobulin fold (26). We have performed superposition of 1IGT with several

high resolution crystal structures of Fab and Fc fragments of human or mouse origins. Since there are no published crystal structure(s) for human IgG2 antibody, we have used human IgG1 crystal structures. The following Fc crystal structures were used: a human IgG1 antibody (PDB ID: 1L6X, 1.65 Å), the human IgG1 therapeutic antibody Herceptin (PDB ID: 3D6G, 2.3 Å), and a mouse IgG2b antibody (PDB ID: 2RGS, 2.1 Å). The Fab crystal structures used were the human IgG1 therapeutic antibody Campath (PDB ID: 1CE1, 1.9 Å) and the mouse IgG2a therapeutic antibody Orthoclone (PDB ID: 1SY6, 2.1Å). The C_α RMSD values between Fab or Fc of 1IGT and the above listed crystal structures are within 2.5 Å. If only C_L, C_H1 or C_H2 are considered, the C_α RMSD values fall below 2.0 Å. The strong structural conservation even without the accompanying strong sequence conservation in Immunoglobulin G was recognized early by Dorrington (27).

Molecular Dynamics Simulation Setup

The Hinge^{++} was used as the starting structure for molecular dynamic simulations. The N and C termini of all four chains were acetylated and amidated, respectively, to neutralize terminal charges. Hinge^{++} was solvated with TIP3P model water in a cubic box (28). The size of water box was chosen such that the minimum distance between solute and its periodic image is greater than the cut-off for potential energy calculation throughout the simulation. Eight Cl^- ions were added to neutralize the system. The total number of atoms in the simulation system ranged from 138,151 to 140,179.

All dynamic simulations were performed using NAMD simulation package (http://www.ks.uiuc.edu/Research/namd/) (29) and AMBER99 all-atom forcefield (30). Both AMBER and CHARMM forcefields have been used extensively in protein simulations. These forcefields were also used in the recently reported full-length antibody simulations. Brandt *et al.* have used AMBER99 and its variant AMBER99SB to successfully reproduce the hydrodynamic properties of an IgG antibody (31). In the simulations conducted by Chennamsetty *et al.*, CHARMM was used to study the aggregation-prone regions in IgG antibody (32). Due to the computationally demanding nature of our simulations, an in-depth evaluation of the effect of different forcefields on Hinge^{++} dynamics was not conducted. However, our MD simulations on a full-length IgG2 mAb using CHARMM forcefield and implicit solvation showed very similar overall dynamical features as Hinge^{++} (data not shown).

The system was first subjected to 20,000 steps of energy minimization with all solute heavy atoms fixed followed by 5,000 steps of energy minimization without any restraints. Equilibration run was then performed for 1 nanosecond (ns). The temperature, pressure, and energy profiles of the system were examined to assure that equilibration was achieved before the start of the production run. The isothermal-isobaric (NPT) ensemble at $T=298$ K and $P=1$bar was used in all equilibration and production runs. The initial velocities were generated from Maxwell-Boltzmann distribution for the equilibration run. All bonds involving hydrogen atoms were restrained and a 2.0 femto-second (fs) integration time step was used in all simulations. Periodic boundary conditions were employed. A cut-off of 12 Å was applied to non-bonded interactions with switch starting at 10 Å. Non-bonded atom pairs were searched within 13.5 Å and were updated every 10 time steps. Particle mesh ewald summation was performed at every other step for long range electrostatic interactions.

All Cys pairs in the simulation system were set in either disulfide-bonded or reduced forms at the beginning and were kept the same in all simulation steps starting from minimization to production run. For Cys pairs in the disulfide-bonded form, the disulfide bond was constrained throughout the simulation, just like the other covalent bonds. The canonical IgG2 disulfide bonding scheme (A-form) was followed for all bonded Cys residues in all simulations. For the reduced form, the disulfide bonds were broken and the Cys side-chain sulphur atoms were reduced by adding the hydrogen atoms to yield–SH groups. There were no constraints on the Cys residue pairs in the reduced form.

Four different sets of independent molecular dynamics simulations were performed. In each set, we obtained two MD simulation trajectories. These four sets of simulations are listed as follows:

1. Control: All intra- and inter- chain Cys residue pairs were disulfide bonded as in canonical IgG2-A form. The two independent simulations are 20 ns long.
2. All-reduced: All intra- and inter- chain disulfide bonding Cys residue pairs were reduced. Two 40 ns independent simulations were performed.
3. Six-reduced: The Cys residue pairs in the two LC. Cys214-HC.Cys128 disulfide bonds and the four inter-HC disulfide bonds in the hinge region were reduced. All the rest of the six Cys residue pairs were kept intra-chain disulfide bonded. Two independent 20 ns simulation trajectories were obtained.
4. Four-reduced: The Cys residue pairs in the two LC. Cys214-HC.Cys128 disulfide bonds and two inter-HC disulfide bonds in the upper hinge region (Cys236-Cys236 and Cys237-Cys237) were reduced. The rest of the eight Cys pairs were in disulfide bonded form. Two independent 20 ns simulation trajectories were obtained.

In all eight simulations, the atomic coordinates were saved every 10 picoseconds (ps) during the production run

for analysis. The length of simulation refers to the duration of production run. An identifier "1" or "2" is used after the simulation name to refer to the two independent simulations in the set. The accumulated simulation time from the eight simulations is 200 ns. On a 32 CPU cluster, 1.5 computer days were required to simulate 1 ns of Hinge^{++} system dynamics.

RESULTS

Brief Description of Hinge^{++} Molecular System and MD Simulations

Hinge^{++} was obtained by truncating a full mouse IgG2a antibody whose core hinge region was replaced with the core hinge region found in human IgG2 mAbs (see Materials and Methods). The truncation involved the removal of Fv and C_H3 domains. Hinge^{++} contains four structural regions, namely, tFab1, tFab2, hinge and tFc (Fig. 1a). tFab1 and tFab2 are the truncated Fabs containing only the constant regions. Similarly, tFc contains only the C_H2 domains of both heavy chains. The sequence location of the hinge region follows Harris *et al.* (24) and contains residues from Glu226 to Gly250 in both heavy chains (Fig. 2a). We follow a hierarchical system to denote individual residues. For example, Cys 214 of light chain 1 is represented as LC1.Cys214.

Four sets of simulations have been performed. Each set contains two independent simulation trajectories. A different number of Cys residue pairs was set in either reduced or disulfide bonded form in these simulation sets. These simulations were named as Control, All-reduced, Six-reduced and Four-reduced, as described in the Materials and Methods section. The time series of the temperature, total energy, volume and averaged pressure of the simulation system are presented in Figure S1 in Supplementary Material. It shows that the equilibrium condition is well-maintained during the production runs.

Overall Conformational Change

For each simulation, the conformational change was estimated by the Root Mean Square Deviation (RMSD) from the starting structure. Figure 3a plots the C_α RMSD profiles of Hinge^{++} for the duration of all eight simulations. The evolution of RMSD profiles is consistent in all trajectories. To assess the structural convergence in our simulations, a quantitative variance analysis of RMSD profiles for all eight simulations is presented in Table S1 in Supplementary Material. Table S1 shows the average, standard deviation and coefficient of variation (ratio of standard deviation to the average) values for the RMSD profiles in the simulation time intervals of 5 ns. The RMSD values increase initially but stabilize at the later stages of the simulations. The standard deviation of RMSD values after 5ns is generally less than 0.8 Å for all simulations except the Six-reduced1. The coefficient of variance after the first 10ns ranges from 0.02 to 0.07 in all simulations. After the first 5 ns time interval, the increase in the average RMSD values across different time intervals is less than 2 Å. All-reduced simulations take longer time to reach this stage. Hinge^{++} is a large (670 residues) multi-domain molecular system. The average RMSD increase of 2–3 Å is quite nominal for such a system.

The plateau in overall RMSD profiles indicates conformational convergence of the molecule. It should not be used to interpret system equilibration. Discarding the production run data prior to RMSD convergence can overestimate the system relaxation time, and valuable information on molecular dynamic behavior may also be lost (33). Schmid *et al.* have used the full production run trajectories for analysis of disulfide scrambling in bovine α-lactabumin, even though their RMSD time series did not converge until the later stages (20). We have also used full production run data for our analysis. Even if we were to discard the first 5 ns in all the simulation trajectories, our observations and conclusions would remain unchanged.

The evolution and the range of the overall RMSD values indicate that the Hinge^{++} undergoes domain motions. We have computed C_α RMSD of each domain in Hinge^{++} to identify the flexible regions and also to identify the reasons behind the overall RMSD change. The overall behavior of domain-wise RMSD is similar in all eight trajectories. Figure 3b and c present domain-wise RMSD profiles for the Six-reduced1 and Control1 simulations, respectively, to serve as examples. The tFab1 and tFab2 domains are stable over the entire simulation. The RMSD values for these two domains remain nearly constant in all simulations. In contrast, the RMSD of tFc increases significantly (RMSD range: 2.2 to 13.4 Å in the Six-reduced1 simulation). tFc consists of C_H2 domains from both heavy chains. The RMSD values of the individual C_H2 domains vary in much smaller range (1.3 to 3.4 Å, not shown in figures). These observations suggest that the interfacial-packing of the two individual C_H2 domains is not maintained during the simulations. This is likely to be an artifact of truncation of Fc domain.

C_α RMSD for the hinge region increases in all simulations, although less significantly than that for tFc. The hinge region is also much smaller in size compared with tFc. The variation of the hinge region C_α RMSD is similar in all the simulations. No significant differences are observed between the control simulations and other simulation sets. Hence, the backbone flexibility of the hinge region does not correlate with the number of inter-chain disulfide bonds in this region.

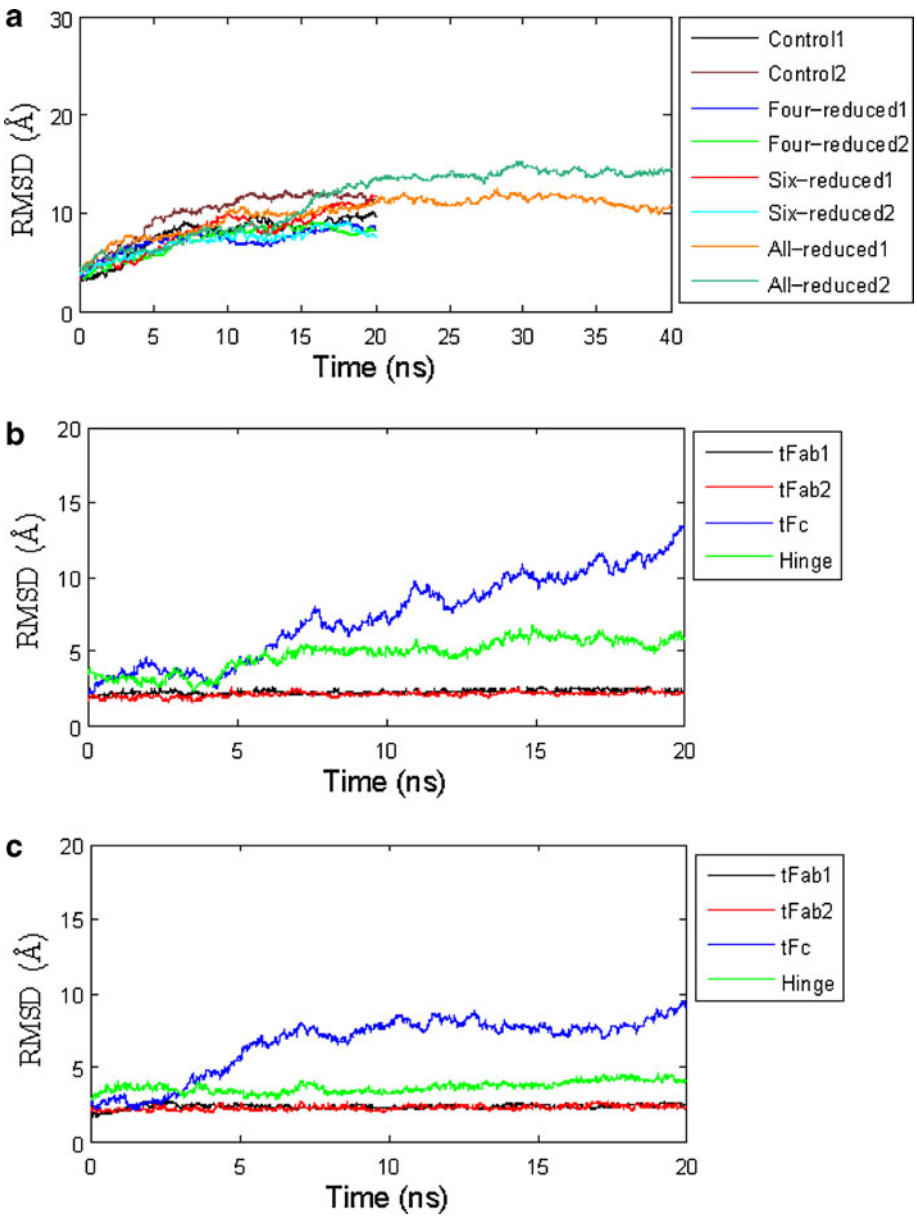

Fig. 3 Time series of C_α RMSD are shown. (**a**) Overall RMSD of the Hinge^{++} for all eight simulations. (**b**) Domain-wise RMSD from the Six-reduced1 simulation. The Hinge^{++} is divided into four domains, namely, tFab1, tFab2, hinge and tFc. (**c**) Domain-wise RMSD from the Control1 simulation.

The radius of gyration (R_g) for Hinge^{++} decreases over time for all simulations (Figure S2 in Supplementary Material). This observation indicates that the molecular system contracts during the simulation, due to movement of tFab and tFc domains towards each other. The inter-domain contacts formed between tFab and tFc were studied to understand these domain motions. Figure 4 shows the number of contacts formed between tFab2 and tFc over simulation time. In our definition, two residues belonging to different regions form a contact if the minimum heavy atom distance between the two residues is within a 5 Å cut-off value. The choice of cut-off distance is arbitrary. We have also tried a cut-off distance of 8 Å. The number of observed contacts increased, but the trend showing the change in number of contacts over time remained similar to that from the 5 Å cut-off. In general, the number of tFab2–tFc contacts increase with time in all simulations except the Six-reduced2. The insert in Fig. 4a shows a snapshot from Four-reduced1 simulation as a representative conformation. Most of the contacts are formed between different heavy chains, i.e., between HC2.C_H1 (in tFab2) and HC1.C_H2 (in tFc). In contrast to tFab2–tFc contact, the contacts between tFab1 with tFc are rare in all simulations. These observations indicate that the motions of the two tFabs are asymmetric in relation to tFc.

Early Events in Disulfide Scrambling

Chemical bonds cannot be made or broken during MD simulations. Hence, the indicators for disulfide scrambling

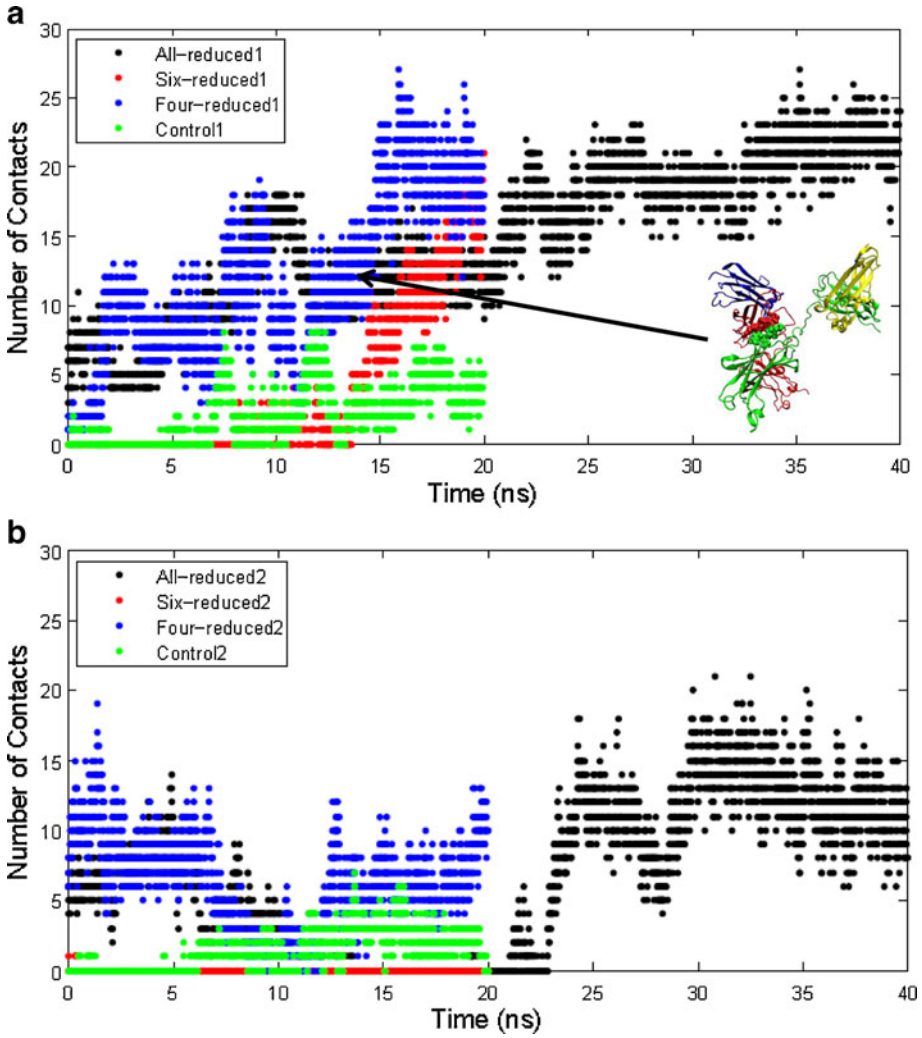

Fig. 4 Number of contacts formed between tFab2 and tFc domains is plotted as function of simulation time. Two residues from different domains are taken to be in contact if at least one pair of heavy atoms from these residues is within 5 Å. (**a**) First trajectories from the four simulation sets are shown (see Materials and Methods section). Insert shows a snapshot from the Four-reduced1 simulation at time 14.5 ns. The yellow, blue, green and red colors indicate LC1, LC2, HC1, and HC2 respectively. The contacting residues are shown in CPK representation. (**b**) Second set of simulations in the four disulfide-bonded conditions.

are limited to the observation of molecular conformation snapshots where the sulphur atoms from non-canonical pair (s) of Cys residues come into close proximity. This method was also used by Schmid *et al.* and Allison *et al.* to study disulfide scrambling in α-lactalbumin and lipid transfer proteins, respectively (20, 21).

Table I lists the average sulphur atom distance for the canonical Cys residue pairs in reduced form. These

Table I Average Sulphur Atom Distance for Cysteine Pairs in Reduced Form (Å)

Number	Cysteine Pair	All-reduced1	All-reduced2	Six-reduced1	Six-reduced2	Four-reduced1	Four-reduced2
1	LC1.C134–LC1.C194	3.7 ± 0.3	3.8 ± 0.3				
2	LC2.C134–LC2.C194	3.7 ± 0.3	3.7 ± 0.2				
3	HC1.C142–HC1.C208	3.9 ± 0.4	3.9 ± 0.4				
4	HC2.C142–HC2.C208	3.8 ± 0.3	3.8 ± 0.3				
5	HC1.C274–HC1.C340	3.7 ± 0.3	3.7 ± 0.3				
6	HC2.C274–HC2.C340	3.8 ± 0.3	3.7 ± 0.4				
7	LC1.C214–HC1.C128	9.2 ± 1.1	7.5 ± 1.9	6.6 ± 0.7	7.0 ± 0.4	4.1 ± 0.7	5.4 ± 1.6
8	LC2.C214–HC2.C128	4.0 ± 0.4	5.5 ± 1.6	5.5 ± 0.9	6.2 ± 1.9	7.7 ± 1.0	7.9 ± 1.7
9	HC1.C236–HC2.C236	7.9 ± 0.8	5.1 ± 1.2	5.8 ± 1.9	12.0 ± 1.3	16.8 ± 5.0	4.7 ± 0.9
10	HC1.C237–HC2.C237	6.8 ± 1.2	6.1 ± 1.3	6.8 ± 1.1	7.5 ± 0.9	8.7 ± 2.8	5.0 ± 1.1
11	HC1.C240–HC2.C240	11.9 ± 1.2	8.3 ± 1.2	7.8 ± 1.7	12.0 ± 1.5		
12	HC1.C242–HC2.C242	8.6 ± 2.1	7.0 ± 1.4	5.0 ± 1.3	8.5 ± 2.1		

distances are relatively short (3.7–3.9 Å) and stable for the intra-chain disulfide bond-forming Cys residue pairs (top 6 in Table I). In contrast, these distances are longer (4–17 Å) and show greater variations for the Cys residue pairs involved in the canonical inter-chain disulfide bonds (bottom 6 in Table I). This observation is consistent with solvent accessible surface area (SASA) values of the Cys residues in the starting structure (Table II). The inter-chain disulfide bond-forming Cys residues have greater average SASA (27.2 ± 19.6 Å^2 , bottom 6 in Table II) than those involved in intra-chain disulfide bonds (0.6 ± 1.3 Å^2, top 6 in Table II). These results indicate the sulphur atoms of inter-chain disulfide bond-forming Cys residues are highly mobile and liable to disulfide scrambling.

Both IgG2-B and IgG2-A/B disulfide isoforms involve the disulfide linkage of LC.Cys214 and/or HC.Cys128 in Fab with the Cys residues in the hinge region. Close sulphur atom proximity is necessary for any two Cys residues to become disulfide-linked. Figure 5a shows the evolution of sulphur distance for the non-canonical Cys pair (LC2.Cys214-HC2.Cys236) over simulation time from the first trajectories in the four sets of simulations. Data for the second trajectories are presented in Figure S3a in Supplementary Material. This distance is 15.3 Å initially and decreases generally over time in all simulations except Control2. This result is consistent with the observation that tFab2 approaches tFc and the number of contacts between the two regions increases over the simulation time (Fig. 4). The insert in Fig. 5a shows a snapshot at 11.5 ns from the Six-reduced1 simulation as an example. The two sulphur atoms are as close as 6.4 Å.

Table II Solvent Accessible Surface Area of Cys Residues in the Starting Structure

Number	Cysteine	SASA (Å^2)	Cysteine	SASA (Å^2)
Intra-chain disulfide bonds				
1	LC1.C134	0.6	LC1.C194	0.5
2	LC2.C134	0.5	LC2.C194	4.5
3	HC1.C142	0.0	HC1.C208	0.0
4	HC2.C142	0.0	HC2.C208	0.0
5	HC1.C274	0.5	HC1.C340	0.0
6	HC2.C274	0.0	HC2.C340	0.0
Inter-chain disulfide bonds				
7	LC1.C214	11.0	HC1.C128	42.5
8	LC2.C214	27.5	HC2.C128	11.4
9	HC1.C236	45.9	HC2.C236	57.7
10	HC1.C237	56.0	HC2.C237	21.4
11	HC1.C240	32.7	HC2.C240	8.5
12	HC1.C242	0.8	HC2.C242	10.9

In the same simulation, their distance drops again below 8 Å at 12.8 ns. These two sulphur atoms come close in the two All-reduced simulations also. Their distance becomes shorter than 8 Å at 9.5, 28.9 and 29.6 ns in the All-reduced1 simulation. Similar events also occurred 10 times in the All-reduced2 simulation (Figure S3a). In the two Four-reduced simulations, this distance increases at the beginning but starts dropping after 10 ns and falls below the initial value by the end of simulation. This distance fell below 10 Å 16 times during 9–16 ns in the Control1 simulation.

HC2.Cys128 also moves in along with LC2.Cys214 towards HC2.Cys236. The time series of the HC2.Cys128-HC2.Cys236 sulphur distance are shown in Fig. 5b and Figure S3b. In the Four-reduced2 and Six-reduced2 simulations, the two sulphur atoms become close (< 10 Å) in later stages of the simulations (Fig. 5b). The insert in Fig. 5b is the snapshot from the Four-reduced2 simulation at 8.7 ns when the distance is 8.3 Å. In the Six-reduced2 simulation, the HC2.Cys128-HC2.Cys236 sulphur distance falls below 10.0 Å several times after 10 ns and reaches a minimum of 6 Å close to the end.

Besides HC2.Cys236, we also explored the close proximity of other hinge region Cys residues with LC2.Cys214 and/or HC2.Cys128. The sulphur atom distances between LC2.Cys214 / HC2.Cys128 and the other hinge region Cys residues mostly remain farther than 10 Å during all simulations. However, a few instances of close proximity were observed. (i) The minimal LC2.Cys214-HC2.Cys237 sulphur atom distance is 9.6 Å in All-reduced1 simulation. (ii) The LC2.Cys214-HC1.Cys236 sulphur atom distance reaches values of 8.6 Å and 9.2 Å in the All-reduced2 and Control1 simulations, respectively. (iii) The HC2.Cys128-HC1.Cys236 and HC2.Cys128-HC1.Cys237 sulphur atom distances touch the minimal values of 8.3–8.9 Å during both Four-reduced simulations. (iv) The HC2.Cys128-HC2.Cys237 sulphur atom distance drops below 10 Å towards the end of the Six-reduced2 simulation accompanied by the drop in HC2.Cys128-HC2.Cys236 distance (Fig. 5b).

While the conformational fluctuations bring LC2.Cys214 and HC2.Cys128 in tFab2 close to the hinge region Cys residues, similar events are not observed for the corresponding Cys residues in tFab1. The average and minimum sulphur atom distance for LC1.Cys214 and HC1.Cys128 with HC.Cys236 are listed in Table III. It can be seen that the corresponding sulphur atom distances of LC1.Cys214 and HC1.Cys128 to Cys236 residues are always greater than 10 Å over entire simulation times in all simulations with only two exceptions. One such exception was observed in the Six-reduced1 simulation where the minimum HC1.Cys128-HC1.Cys236 sulphur atom distance is to 9.9 Å (at 8.6 ns). In the Control2 simulation,

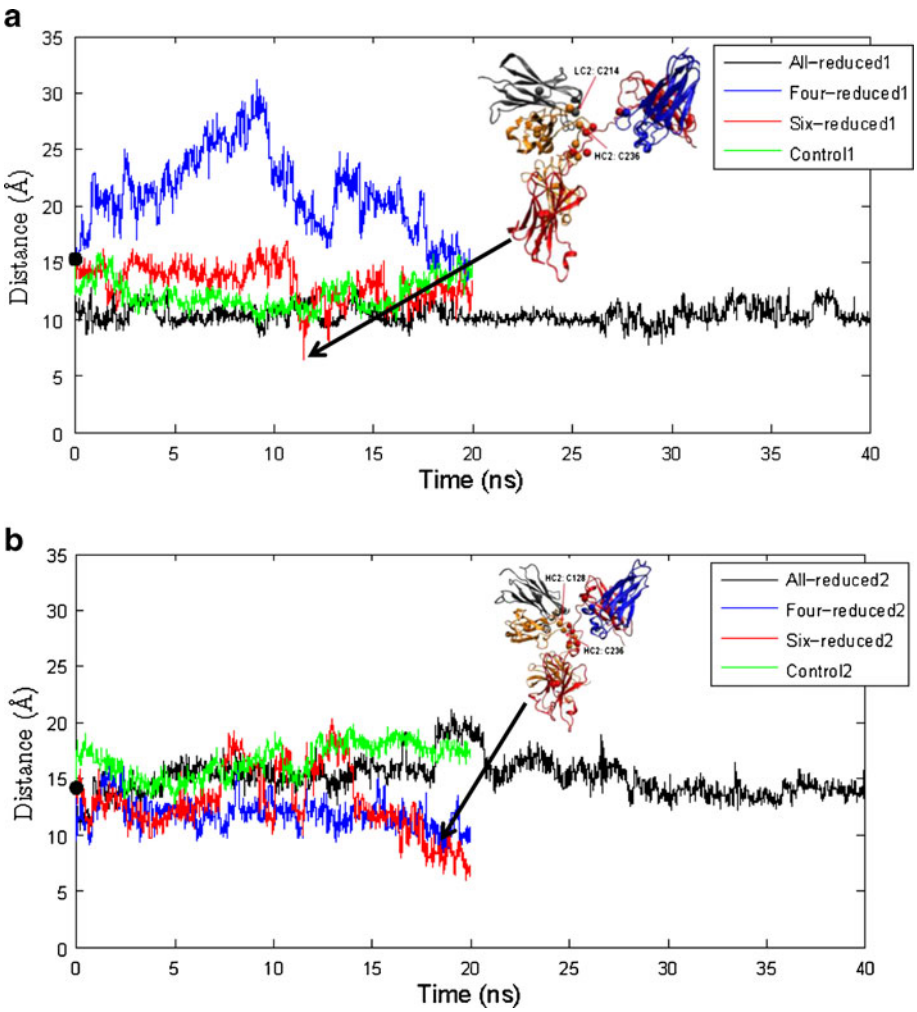

Fig. 5 Time course plots for (**a**) LC2.C214-HC2.C236 sulphur atom distance in the first trajectories from the four simulation sets. The solid black circle at time 0 indicates the initial distance. The inset shows a snapshot from the Six-reduced1 simulation at 11.5 ns. Chains are shown in cartoon representation. All sulphur atoms in Cys residues are shown in CPK representation. (**b**) HC2.C128-HC2.C236 sulphur atom distance in the second trajectories from the four simulation sets. The inset shows a snapshot from the Four-reduced2 simulation at 8.7 ns. Representations for chains and sulphur atoms are same as in Fig. 5a.

the HC1.Cys128-HC2.Cys236 sulphur atom distance drops below 10 Å once (9.6 Å at 10.6 ns). The sulphur atom distances of Cys214 and Cys128 in tFab1 from the hinge Cys residues other than HC.Cys236 are always greater than 13 Å in all simulations.

Hinge Region Dynamics and Non-Canonical Disulfide Linkage

The motion of a Cys residue with respect to other Cys residues in the hinge region may play an important role in

Table III Sulphur Atom Distance Between Cys Residues in tFab1 and Cys236 Residues in the Hinge Region

Cysteine Pair	Value (Å)	Control1	Control2	All-reduced1	All-reduced2	Six-reduced1	Six-reduced2	Four-reduced1	Four-reduced2
LC1.C214–HC1.C236	Minimum	11.9	11.4	11.8	13.7	12.8	10.9	13.8	16.7
	Mean	15.5 ± 1.1	15.4 ± 1.2	14.9 ± 1.0	16.7 ± 0.9	16.3 ± 1.2	15.4 ± 1.6	19.0 ± 1.9	21.0 ± 1.4
LC1.C214–HC2.C236	Minimum	12.4	10.9	13.6	15.7	16.4	20.8	18.5	20.3
	Mean	16.2 ± 1.2	15.7 ± 1.3	18.5 ± 1.2	19.8 ± 1.2	20.2 ± 1.3	24.5 ± 1.5	25.6 ± 2.9	24.1 ± 1.2
HC1.C128–HC1.C236	Minimum	11.4	10.2	17.5	17.4	9.9	10.7	14.6	16.8
	Mean	15.1 ± 1.3	14.1 ± 1.2	22.4 ± 1.2	21.9 ± 1.6	14.4 ± 1.6	14.2 ± 1.1	20.3 ± 2.8	21.4 ± 1.3
HC1.C128–HC2.C236	Minimum	11.7	9.6	21.4	19.4	15.2	20.2	18.4	20.6
	Mean	15.6 ± 1.3	14.2 ± 1.3	26.5 ± 1.5	24.8 ± 1.7	19.4 ± 1.5	25.1 ± 1.1	25.7 ± 2.9	24.7 ± 1.4

formation of potential non-canonical disulfide linkages. The hinge region in antibodies is highly dynamic and, thus, poorly defined in all the three publicly available crystal structures of full-length antibodies (1IGY, 1IGT and 1HZH). In case of 1IGT, average B factor value for the hinge region backbone atoms is 120 $Å^2$. The corresponding average B-value for all the backbone atoms in 1IGT is 49 $Å^2$. The variations in C_α virtual torsion angles can also yield clues to the local hinge region dynamics. C_α virtual torsion angle is defined as the dihedral angle formed by (i-1)–i–(i + 1)–(i + 2) C_α atoms. Figure 6 shows the Root Mean Squared Deviation (RMSD) of C_α virtual torsion angles from the starting structure for two representative simulations (Control1 and All-reduced1). The residues flanking the hinge region are also shown in Fig. 6 for comparison. The C_α virtual torsion angle RMSD profiles are similar for both Control1 (Fig. 6a) and All-reduced1 (Fig. 6b). The hinge region residues in both the heavy chains show remarkable deviation as compared with their neighbors. The other simulation trajectories also show similar behavior. These observations are consistent with the expected high mobility of the hinge region.

Inter-Cys contact map is a convenient way to present motions of multiple Cys residues. The contact maps for the eight Cys residues in the hinge region are shown in Fig. 7 for the first trajectories in the four simulation sets. The rest of the data are presented in Figure S4. Two Cys residues are considered to be in contact if their sulphur atoms are within 5 Å. We have followed a non-traditional way to plot these contact maps. Note that the order of the eight hinge region Cys residues along the X-axes (four Cys residues in HC1 followed by the four Cys residues in HC2) is opposite to that along the Y-axes (the four Cys in HC2 are followed by four Cys in HC1) in these contact maps. We chose this representation because the diagonals now represent the in-register inter-HC Cys contacts involved in the canonical disulfide bonds. The off-diagonal contacts involve non-canonical Cys residue pairs. The contact map can be divided into four quadrants. The intra-HC contacts reside in the top left and bottom right quadrants. The inter-HC Cys contacts are shown in the remaining two quadrants.

The contact map for the Control simulations (Fig. 7a and Figure S4a) clearly shows that the diagonal contacts are the dominant ones. This is because the hinge Cys residues

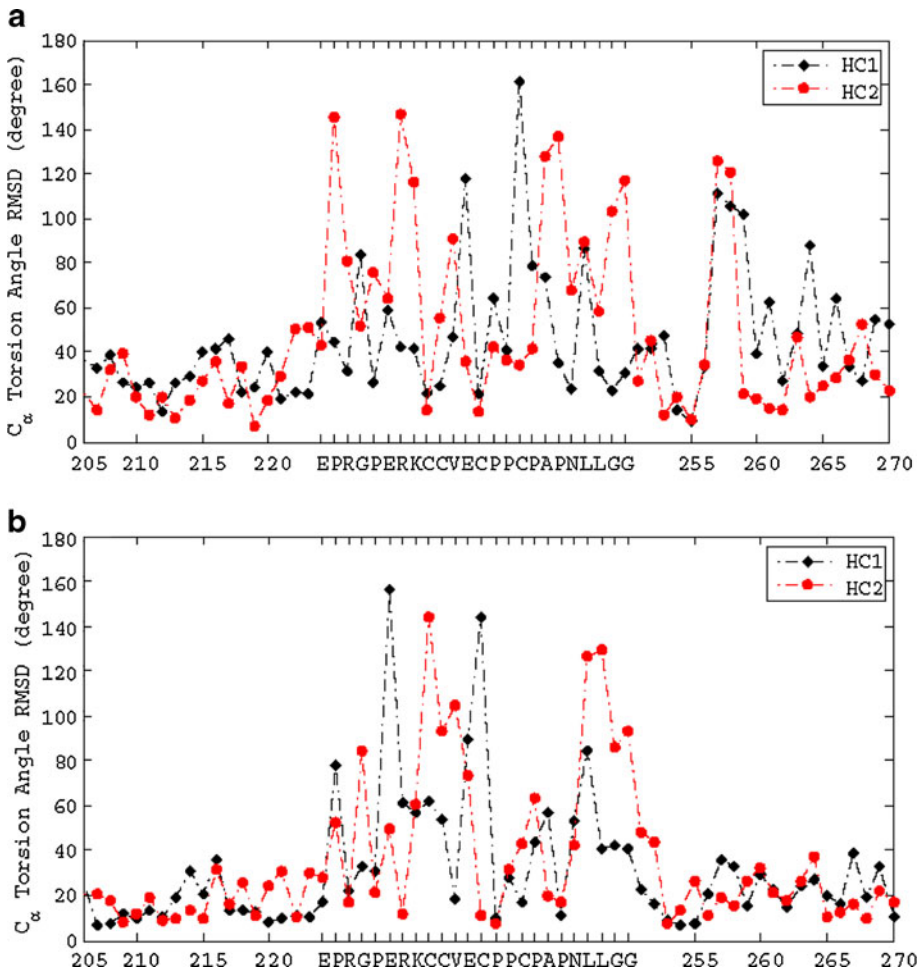

Fig. 6 Root mean squared deviation (RMSD) of C_α virtual torsion angles from the starting structure for the hinge and flanking region sequences in the two heavy chains (HC1 and HC2). C_α virtual torsion angle is defined as the dihedral angle formed by (i-1)–i–(i + 1)–(i + 2) C_α atoms. Names of residues in hinge region are labeled in X-axis. The flanking residues are labeled by Kabat residue numbers. (**a**) Control1 simulation; (**b**) All-reduced1 simulation.

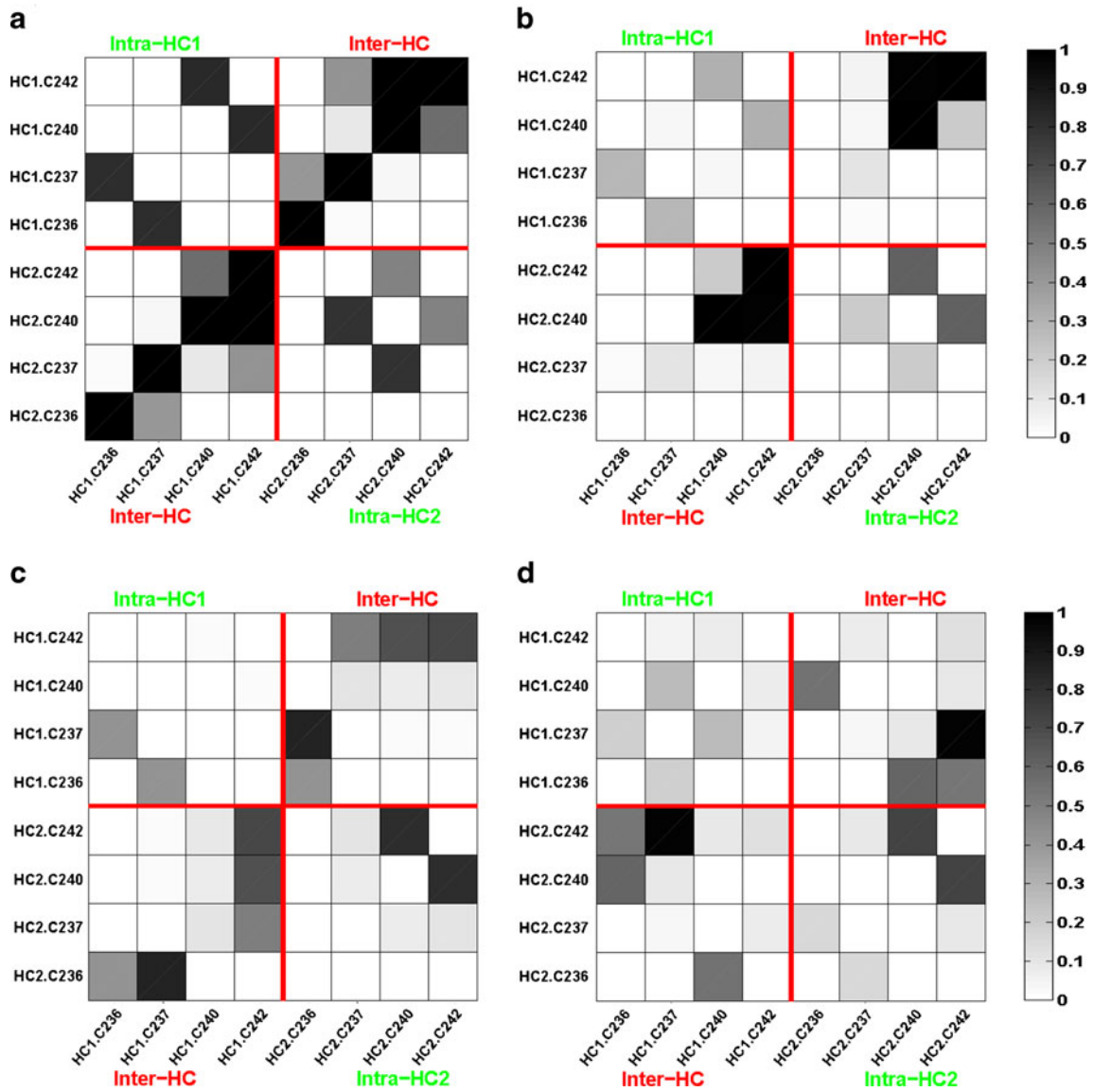

Fig. 7 Contact maps for the eight Cys residues in the hinge region in (**a**) Control1 simulation; (**b**) Four-reduced1 simulation; (**c**) Six-reduced1 simulation; and (**d**) All-reduced1 simulation. Gray scale indicates the frequency of observing a given Cys-Cys contact. A contact is defined by sulphur atom distance for two Cys residues being <5 Å. Note that the order of Cys residues along X- axis is opposite to that along the Y-axis. Each quadrant is labeled according to the nature of contacts. Inter-heavy chain contacts (inter-HC) are located in upper right or lower left quadrants. Intra-heavy chain contacts (Intra-HC1 and Intra-HC2) reside in the other two quadrants.

are disulfide bonded in this simulation. However, off-diagonal contacts are also frequent, including both intra- and inter-HC contacts. When some or all the inter-chain disulfide bonds are reduced, the diagonal contacts become less prevalent as shown in the contact maps of the Four-reduced1, Six-reduced1 and All-reduced1 simulations (Fig. 7b,c,d). Results from the remaining simulations (Figure S4) are similar. In all simulations with reduced disulfide bonds, there is no clear evidence in favor of either intra-HC or inter-HC Cys residue contacts. Moreover, there is no clear preference for either in-register contacts or out-of-register inter-HC contacts. The contacts across the upper (KCCVE) and lower (CPPCP) portions of the hinge region are also observed. However, these contacts are less frequent than the contacts within either the upper hinge or the lower hinge regions. A non-canonical disulfide bond formed between Cys residues in the lower hinge has been experimentally detected by Zhang *et al.* (12).

DISCUSSION

Recent path-breaking experimental studies have documented disulfide scrambling in human IgG2 mAbs (8, 9,

18). It has been shown that inter-chain disulfide bonds in human IgGs are susceptible to exchange in presence of redox potential, such as in human blood, (10) and also during the commercial production of therapeutic IgG2 and subsequent purification steps (8). Due to the importance of antibody-based therapeutics, a fundamental understanding of antibody structure-function relationships is essential, including an understanding of the reasons behind the variation in the covalent structure of antibodies. Moreover, the *in vivo* instability of hinge region inter-chain disulfide bonds could have important consequences for pharmacokinetic / dynamic properties of mAb-based therapeutics (6). Our molecular dynamics simulations have attempted to provide atomistic details about the hinge region instability in the human IgG2 mAbs. These insights are consistent with the experimental observations made so far. They also supplement our understanding of the molecular events that lead to disulfide scrambling in the IgG2 mAbs. In this study, we have devised a molecular model system, $Hinge^{++}$, to represent the middle portion of human IgG2 antibody. $Hinge^{++}$ is derived from the crystal structure of a full-length murine IgG2a mAb with kappa light chain. The core hinge region of this antibody was tweaked to that found in the human IgG2 mAbs *via* molecular modeling. Potential errors due to modeling were minimized as we retained more than 99% of the 1IGT crystal structure.

We have performed explicit water multiple dynamics simulations on $Hinge^{++}$ to uncover dynamical features that may initiate disulfide scrambling. Due to the large size of the molecular system, these explicit water simulations are computationally expensive. $Hinge^{++}$ is de-glycosylated and truncated from full-length antibody to speed up the simulations, while maximally preserving the structural domains relevant to disulfide scrambling. In a separate study, we have performed simulations on both glycosylated and un-glycosylated forms of full-length murine antibody contained in the PDB entry 1IGT (our unpublished work). These simulations are analogous to the Control simulations in this study. The dynamical natures of the hinge regions are very similar in full length and truncated molecular systems. Upon removal of C_H3 domains and upon de-glycosylaion, the individual C_H2 domains remained stable, but the association of the two C_H2 domains became weaker. These effects are restricted to C_H2 domains and do not impact other domains and the hinge region. Eight independent simulations with different numbers of broken disulfide bonds were performed. The cumulative simulation time is 200 ns. Each simulation is at least 20 ns. We expected that $Hinge^{++}$ system in the All-reduced simulations shall be most flexible due to the lack of all inter- and intra-chain disulfide bonds. Hence, we had extended the two All-reduced simulations to 40 ns to ensure good conformational convergence. We have analyzed the two All-reduced simulations based on the first 20 ns and the whole 40 ns of the trajectories. Our results did not change due to the extension of the simulation from 20 ns to 40 ns. Our simulations are also of comparable duration as the other published works on IgG molecules. Brandt *et al.* have computed the hydrodynamic properties of a full IgG antibody based on 40-ns long simulations (31). In another example, Chennamsetty *et al.* have used a 30 ns MD simulation of an IgG antibody to identify surface-exposed hydrophobic patches as aggregation-prone motifs (32).

We have computed two trajectories for each of the four simulation sets. The details of atomic motions observed in different trajectories are expected to vary because of the underlying stochastic nature of molecular dynamics simulations. However, several trends were consistently observed across different simulation trajectories. 1) The sulphur atom distances for intra-chain disulfide bond-forming Cys pairs are short and stable (Table I, top 6 lines), while those for inter-chain disulfide bond-forming Cys pairs are large and fluctuate significantly (Table I, bottom 6 lines). 2) The overall RMSD profiles of all the eight simulations (Fig. 3a) are very similar. 3) All simulations consistently show that tFab2 and tFc move towards each other in the early stages. 4) The number of tFab2–tFc contacts (Fig. 4) generally increases with time in all simulations. The analogous tFab1–tFc interaction is rare in all the trajectories. 5) Because of the proximity of tFab2 with tFc, we observed frequent proximity between LC2.C214 and HC2.C236 (Fig. 5). Consistently, all simulations indicate that the proximity of LC1.C214 with HC.Cys236 is rare (Table III). 6) The inter-HC in-register Cys-Cys contacts in the hinge region are not the preferred ones under reducing conditions. All simulations show that inter-HC non-register and intra-HC Cys-Cys contacts in the hinge region are feasible. 7) The molecular conformations become compact indicated by smaller Rg (Figure S2) in all simulations. The Rg profiles of the 20 ns-long simulations do not plateau. However, they are expected to follow the same trend as shown by the Rg profiles of the two All-reduced 40 ns-long simulations. 8) The simulations with broken disulfide bonds behave similarly to the control simulations, indicating that intra- and inter-chain packing of an IgG antibody is mainly maintained by strong non-covalent interactions. This was also suggested by the experiments of Dorrington (27).

The hinge region is highly dynamic, and it is conceivable that random motions could also place these sulphur atoms in close spatial proximities. Sulphur atom proximity is a necessary but not sufficient condition for disulfide scrambling. Other stereo-chemical factors such as side-chain rotamer variation can also play a role in the formation of disulfide bonds. A limitation of molecular dynamics is that one cannot make or break chemical bonds during the

course of simulations. In literature, the repeated close approach of sulphur atoms from Cys residue pairs in MD simulations has been used to indicate potential for disulfide exchange (20, 21). The consistently observed repeat close proximities between the sulphur atoms from non-canonical Cys pairs in our simulations cannot be explained by purely random motions. In particular, our simulations show that LC2.C214 and LC2.C128 repeatedly become close to Cys residues in upper hinge region (HC.C236). This is due to the domain motion of Fab2 towards Fc and highly dynamic nature of antibody hinge region. Furthermore, our results are consistent with the disulfide isoforms proposed from the experimental studies. The four-reduced simulation set mimics the early experimental evidence for the disulfide scrambling (8, 9). The two inter-HC disulfide bonds in lower hinge region were kept intact in this simulation set. The newer experimental evidence indicates that lower hinge region disulfide bonds may also scramble (12). All-reduced and Six-reduced simulation sets put all eight hinge region Cys residues on even keel and explore disulfide scrambling potential in the hinge region. Our results indicate that the inter-chain disulfide pairings are highly degenerate, and we expect to find experimental examples involving additional Cys residues in the hinge region as research in this area progresses.

How is disulfide scrambling initiated? In the canonical IgG2-A form, the two Fabs are structurally independent of hinge region (Fig. 1a). In contrast, one or both Fabs are disulfide linked to the upper hinge region in the IgG2-B and IgG2-A/B isoforms (8, 9) (Fig. 1b and c). This implies that the Fabs must dynamically interact with the hinge region to facilitate the formation of Fab-hinge region disulfide linkage. It has been known that Fabs possess considerable mobility, enabled by the flexible hinge region (34). Consistent with these experimental reports, all the simulations in this report show increased formation of contacts between tFab2 and tFc as the two domains move towards each other (Fig. 4). The tFab1, however, does not show a similar movement towards tFc. This results in a skewed orientation of the two tFabs with respect to tFc. Consistent with this observation again, Dillon *et al.* had speculated that the oblique orientation of Fabs with respect to Fc positions the two Cys residues in Fab (LC.Cys214 and HC.Cys128) in close proximity with the Cys residues in upper hinge region and facilitates disulfide exchange (8). The Cys214-Cys236 linkage within the half molecule forms the basis for most variants of IgG2-B and IgG2-A/B isoforms reported so far (8, 9, 11, 18). Taking together the results from different experimental studies and the simulations presented here, it appears that the disulfide scrambling is initiated when LC.Cys214 / HC.Cys128 come in close spatial vicinity with HC.Cys236 residues.

In our simulations, the sulphur atom distances for LC2.Cys214-HC2.Cys237, LC2.Cys214-HC1.Cys236, HC2.Cys128-HC1.Cys236 and HC2.Cys128-HC2.Cys237 occasionally drop below 10 Å due to conformational fluctuation. This observation suggests that there is a potential for disulfide bond formations by these Cys residue pairs. Consistently, LC.Cys214 forms disulfide bond with Cys237 of the pairing heavy chain instead of Cys236 in an IgG2-B isoform reported by Martinez *et al.* (11). The IgG2-A/B isoform reported by Dillon *et al.* contains the disulfide bond between LC.Cys214 and Cys236 of the other heavy chain rather than the one that pairs with light chain (8). All these disulfide pairing schemes are consistent with the results of our simulations.

In IgG2-B isoforms, both the Fabs are disulfide linked with the hinge region. In our simulations, potential for disulfide linkage is observed for only one Fab. The other Fab is distant from the hinge in all simulations. There could be two reasons for this: first, the timescales for our simulations are not long enough; second, the two Fabs may not scramble their disulfide bonds with the hinge region simultaneously. This implies that formation of IgG2-A/B isoforms may be an intermediate step during the conversion of IgG2-A isoform to IgG2-B isoforms. Consistently, Liu *et al.* have reported that nascent human IgG2 antibodies produced by the antibody-secreting cells are predominantly of IgG2-A form. While circulating in the blood, These A-form antibodies are first converted to IgG2-A/B form and finally to IgG2-B form (10).

The hinge region is highly mobile as shown by domain C_α RMSD and C_α virtual torsion angle RMSD profiles (Figs. 3 and 6) as well as high B-factors in the crystal structures. As a result, inter-chain disulfide linkages in human IgG can be highly facile and complex. Despite the variations across different simulation trajectories, the hinge Cys residues contact maps from all simulations (Fig. 7 and Figure S4) consistently indicate that human IgG2 mAbs may contain several non-canonical disulfide patterns, in addition to those reported experimentally so far. The contact maps show frequent intra-chain contacts in addition to inter-chain contacts. When all the four inter-chain disulfide bonds in the hinge are reduced, as in the All-reduced and Six-reduced simulations, there is no strong preference for inter-chain Cys contacts over intra-chain ones. Moreover, disulfide bonds linking the upper (KCCVE) and lower (CPPCP) portions of hinge region may also occur. The stereo-chemical requirements may limit the formation of some of the disulfide linkages even if the involved Cys residues are in spatial vicinity (35). Consistently, Zhang *et al.* (2010) have reported a novel variant of IgG2-B which contains an intra-chain disulfide bond formed between the two Cys residues in the lower hinge (CPPCP) (12).

During therapeutic mAb product development, disulfide scrambling contributes to product heterogeneity and

complicates comparability studies. Hence, methods and strategies have been developed to eliminate or mitigate disulfide heterogeneity of human IgG2 mAbs (18, 19, 36). The main approach is to mutate the Cys residues involved in disulfide scrambling. In particular, C128S, C236S and C237S mutations of heavy chain have been experimentally investigated, and the mutants are shown to be structurally homogeneous. Double mutants which combine these Cys residues have also been examined and show similar improvement in structural homogeneity. Our simulation results are consistent with these observations. However, the above stated mutational experiments address the issue only partially. The potential for disulfide scrambling from the lower hinge region is not considered in the previous studies. Another approach to mitigate disulfide scrambling is the kappa light chain (κ LC) extension by adding Ser residue(s) at the C-terminal, like in lambda light chains (λ LC) (18). Other structure-based design strategies that seek to reduce the conformational heterogeneity of the hinge region could also mitigate disulfide scrambling. Our simulations indicate the following additional protein design strategies to reduce or eliminate disulfide scrambling in IgG2 mAbs: (i) mutate the Cys residues to Ser or Ala in the lower hinge region; (ii) eliminate all inter-chain disulfide bonds; (iii) reduce the conformational flexibility of the core hinge region by mutating the non-Cys residues, especially the Val and Glu in the core hinge region (CCVECPPC). While engineering any mutations, one should also consider their potential impact on the Fc-related biological activities of the mAbs.

In conclusion, the inter-chain disulfide bond-forming Cys residues are more mobile than the intra-chain disulfide bond-forming Cys residues. Disulfide scrambling in human IgG2 molecules is limited to inter-chain disulfide bonds. Hinge region dynamics can place the Cys residue pairs in a large number of spatially proximal positions, leading to a several potential non-canonical disulfide bonding schemes. The segmental flexibility enabled by the hinge region also facilitates closer inter-domain contacts, leading to the close proximity of LC.Cys214 and HC.Cys128 in Fab with Cys residues in the upper hinge region. Such events could initiate disulfide scrambling under appropriate conditions. The motions of two Fabs towards Fc are asymmetric in the early stages, implying that IgG2 A/B isoform could be an intermediate of disulfide scrambling. The dynamics of hinge region do not show any preference for the canonical inter-HC in-register disulfide linkage. The non-canonical inter-HC disulfide linkages and intra-HC linkages are also feasible.

ACKNOWLEDGMENTS

We appreciate the anonymous referees for their constructive criticism of the research work and for suggestions to improve the manuscript. We thank Drs. Sandeep Nema, Sa V Ho, James Carroll, B. Muralidhara, Patrick Buck and Kevin King for several helpful discussions and for critical reading of this manuscript. A postdoctoral fellowship for Xiaoling Wang in Biotherapeutics Pharmaceutical Research and Development, Pfizer Inc. is gratefully acknowledged. High Performance Computing Support received from Pfizer Research Informatics played an essential role in this project.

REFERENCES

1. Salfeld JG. Isotype selection in antibody engineering. Nat Biotechnol. 2007;25(12):1369–72.
2. Labrijn AF, Aalberse RC, Schuurman J. When binding is enough: nonactivating antibody formats. Curr Opin Immunol. 2008;20 (4):479–85.
3. Winter G, Duncan A, Burton D. Altered antibodies. USA patent WO-88/07089. Sept. 22. 1988.
4. Jefferis R. Antibody therapeutics:isotype and glycoform selection. Expert Opin Biol Ther. 2007;7(9):1401–13.
5. Beck A, Reichert JM, Wurch T. 5th European antibody congress 2009: November 30–December 2, 2009, Geneva, Switzerland. mAbs. 2010; 2(2):108–28.
6. Labrijn AF, Buijsse AO, van den Bremer ETJ, Verwilligen AYW, Bleeker WK, Thorpe SJ, *et al.* Therapeutic IgG4 antibodies engage in Fab-arm exchange with endogenous human IgG4 *in vivo*. Nat Biotechnol. 2009;27(8):767–71.
7. Aalberse RC, Schuurman J. IgG4 breaking the rules. Immunology. 2002;105(1):9–19.
8. Dillon TM, Ricci MS, Vezina C, Flynn GC, Liu YD, Rehder DS, *et al.* Structural and functional characterization of disulfide isoforms of the human IgG2 subclass. J Biol Chem. 2008;283 (23):16206–15.
9. Wypych J, Li M, Guo A, Zhang Z, Martinez T, Allen MJ, *et al.* Human IgG2 antibodies display disulfide-mediated structural Isoforms. J Biol Chem. 2008;283(23):16194–205.
10. Liu YD, Chen X. Enk JZ-v, Plant M, Dillon TM, Flynn GC. Human IgG2 antibody disulfide rearrangement *in vivo*. J Biol Chem. 2008;283(43):29266–72.
11. Martinez T, Guo A, Allen MJ, Han M, Pace D, Jones J, *et al.* Disulfide connectivity of human immunoglobulin G2 structural isoforms. Biochemistry. 2008;47(28):7496–508.
12. Zhang B, Harder AG, Connelly HM, Maheu LL, Cockrill SL. Determination of Fab-hinge disulfide connectivity in structural isoforms of a recombinant human immunoglobulin G2 antibody. Anal Chem. 2010;82(3):1090–9.
13. Yoo EM, Wims LA, Chan LA, Morrison SL. Human IgG2 can form covalent dimers. J Immunol. 2003;170(6):3134–8.
14. Pink JRL, Milstein C. Inter heavy-light chain disulphide bridge in immune globulins. Nature. 1967;214(5083):92–4.
15. Edelman GM, Cunningham BA, Gall WE, Gottlieb PD, Rutishauser U, Waxdal MJ. The covalent structure of an entire γG immunoglobulin molecule. Proc Natl Acad Sci U S A. 1969;63(1):78–85.
16. Milstein C, Frangione B. Disulphide bridges of the heavy chain of human immunoglobulin G2. Biochem J. 1971;121(2):217–25.
17. Frangione B, Milstein C. Variations in the S–S bridges of immunoglobins G: Interchain disulphide bridges of γG3 myeloma proteins. J Mol Biol. 1968;33(3):893–906.
18. Dillon TM, Bondarenko P, Wypych J, Allen M, Balland A, Ricci Margaret S, et al.; Homogeneous antibody populations. USA patent WO 2009/036209. March 19. 2009.

19. Allen MJ, Guo A, Martinez T, Han M, Flynn GC, Wypych J, *et al.* Interchain disulfide bonding in human IgG2 antibodies probed by site-directed mutagenesis. Biochemistry. 2009;48(17):3755–66.
20. Schmid N, Bolliger C, Smith LJ, van Gunsteren WF. Disulfide bond shuffling in bovine α-lactalbumin: MD simulation confirms experiment. Biochemistry. 2008;47(46):12104–7.
21. Allison JR, Moll G-P, van Gunsteren WF. Investigation of stability and disulfide bond shuffling of lipid transfer proteins by molecular dynamics simulation. Biochemistry. 2010;49(32):6916–27.
22. Harris LJ, Larson SB, Hasel KW, Day J, Greenwood A, McPherson A. The three-dimensional structure of an intact monoclonal antibody for canine lymphoma. Nature. 1992;360(6402):369–72.
23. Berman H, Henrick K, Nakamura H. Announcing the worldwide Protein Data Bank. Nat Struct Mol Biol. 2003;10(12):980–0.
24. Harris LJ, Larson SB, Hasel KW, McPherson A. Refined structure of an intact IgG2a monoclonal antibody. Biochemistry. 1997;36(7):1581–97.
25. Prabakaran P, Vu BK, Gan J, Feng Y, Dimitrov D, Ji X. Structure of an isolated unglycosylated antibody C(H)2 domain. Acta Crystallogr D Biol Crystallogr. 2008;64(10):1062–7.
26. Branden C, Tooze J. Introduction to protein structure: Garland Publishing; 1998.
27. Dorrington K. The structural basis for the functional versatility of immunoglobulin G. Can J Biochem. 1978;56(12):1087–101.
28. William LJ, Corky J. Temperature dependence of TIP3P, SPC, and TIP4P water from NPT Monte Carlo simulations: Seeking temperatures of maximum density. J Comput Chem. 1998;19(10):1179–86.
29. Phillips JC, Braun R, Wang W, Gumbart J, Tajkhorshid E, Villa E, *et al.* Scalable molecular dynamics with NAMD. J Comput Chem. 2005;26(16):1781–802.
30. Cheatham TEI, Cieplak P, Kollman PA. A modified version of the Cornell et al. force field with improved sugar pucker phases and helical repeat. J Biomol Struct Dyn. 1999;16(4):845–62.
31. Brandt JP, Patapoff TW, Aragon SR. Construction, MD simulation, and hydrodynamic validation of an all-atom model of a monoclonal IgG antibody. Biophys J. 2010;99(3):905–13.
32. Chennamsetty N, Helk B, Voynov V, Kayser V, Trout BL. Aggregation-prone motifs in human immunoglobulin G. J Mol Biol. 2009;391(2):404–13.
33. Stella L, Melchionna S. Equilibration and sampling in molecular dynamics simulations of biomolecules. J Chem Phys. 1998;109 (23):10115–7.
34. Schneider WP, Wensel TG, Stryer L, Oi VT. Genetically engineered immunoglobulins reveal structural features controlling segmental flexibility. Proc Natl Acad Sci U S A. 1988;85 (8):2509–13.
35. Sowdhamini R, Srinivasan N, Shoichet B, Santi DV, Ramakrishnan C, Balaram P. Stereochemical modeling of disulfide bridges. Criteria for introduction into proteins by site-directed mutagenesis. Protein Eng. 1989;3(2):95–103.
36. Lightle S, Aykent S, Lacher N, Mitaksov V, Wells K, Zobel J, *et al.* Mutations within a human IgG2 antibody form distinct and homogeneous disulfide isomers but do not affect Fc gamma receptor or C1q binding. Protein Sci. 2010;19(4):753–62.